Inferring stellar ages using a combination of stellar evolution models and gyrochronology

ABSTRACT

The ages of main sequence stars are difficult to infer because their outward appearances change subtly and slowly during their hydrogen burning lifetimes. In the era of *Gaia*, where precise parallaxes are available for millions of stars, isochrone fitting can be used to provide a constraint on stellar ages. In addition, for those stars with observed rotation periods, gyrochronal ages may also be available. By combining two sets of observable stellar properties and dating methods that are sensitive to different evolving processes in stars: isochrone fitting and gyrochronology; it is possible to infer more precise and accurate ages than using either method in isolation. In this investigation, the isochronal observables of main sequence stars ($T_{\rm eff}$, [Fe/H], log g, parallax and apparent magnitudes) are combined with their *Kepler* rotation periods, using a Bayesian framework, to infer their ages as predicted from *both* stellar evolution models and gyrochronology. We show that incorporating rotation periods into isochrone models significantly improves the precision of inferred ages. However, since ages predicted with gyrochronology are, in general, much more *precise* than isochronal ages but not necessarily more *accurate*, care must be taken to ensure either a) the gyrochronology relation being used is *extremely* accurate, or b) its precision is relaxed by introducing a mixture model or some intrinsic scatter or similar. In this pilot study we do not aim to produce a new state-of-the-art dating model, our goal is simply to explore the process of combining two heterogeneous dating methods. Combining methods like this can illuminate flaws in one or both, although without ground truth it can be difficult to identify the cause of inconsistencies. Although calibration is not the main purpose of this exploratory investigation and the parameters of our gyrochronology model are fixed, only a slight modification to our algorithm would be required to perform a calibration. Accompanying this publication is open source, packaged and documented code, that calculates stellar ages from spectroscopic parameters and/or apparent magnitudes, parallaxes and rotation periods.

1. Introduction

The formation and evolution of the Milky Way (MW) and the planetary systems within it are currently two topics of interest in astronomy. Both of these fields require precise and accurate ages of thousands of stars. Recent advances in galactic archaeology have been made using the ages of red giants, some calculated from asteroseismology and some from spectroscopy, to explore the age distributions of stellar populations in the MW (*e.g.* **?**) Red giants are highly luminous and can be observed to great distances, thus providing age information on the scale of tens of kilo-parsecs. Main sequence (MS) stars on the other hand, although fainter, are more numerous and so their ages may provide new insights into the formation and evolution of the Solar neighborhood. MS star ages are also of great interest for studying the formation and evolution of planetary systems. Almost all exoplanets discovered to date orbit MS stars and it is therefore *MS star* ages that are needed to capture snapshots of planet evolution. Unfortunately, the very property that makes MS stars good hosts for habitable planets also makes them difficult to date: they do not change substantially over time.

Unlike the spectra and photometric colors of red giants, MS star spectra and colors do not contain a significant amount of age information because they do not change rapidly with age. This is represented in the spacing of isochrones on a Hertsprung-Russell (HR) or color-magnitude diagram (CMD). On the MS, isochrones are tightly spaced and, even with very precise measurements of effective temperature and luminosity, the position of a MS star on the HR diagram may be consistent with range of isochrones spanning several billion years. On the giant branch however, isochrones are spread further apart, so that sufficiently precisely measured temperatures and luminosities may yield ages that are precise to within 20% or better. Look at typical age uncertainties from APOGEE. Asteroseismology can provide precise ages of both red giant and MS stars but due to the greater abundance of observations suitable for *red giant* asteroseismology, precise red giant asteroseismic ages once again outnumber MS ages. The typical periods of red giant acoustic pulsations are long (on the orders of hours to weeks) and can be detected using *Kepler*'s long cadence mode of one observation per thirty minutes, which is *Kepler*'s most common observing mode. In addition, the amplitudes of red giant pulsations are typically very large, significantly greater than *Kepler*'s photometric noise floor. MS stars, on the other hand, oscillate with periods of just a few minutes and the long cadence *Kepler* observations, taken once every half-hour (which is far above the Nyquist limit) are not capable of resolving these pulsations. Instead, to resolve the pulsation frequencies of MS stars they must be observed in *Kepler*'s short cadence mode of one observation every minute. However, since the amplitude of pulsation scales with stellar radius, the majority of stars with asteroseismic ages successfully measured using *Kepler* short-cadence observations (of which there are currently around 500)

are subgiants. Only a small fraction of these 500 are truly on the MS. How many? This may change soon however: *Kepler*'s short cadence light curves have recently been reprocessed and new, precise ages for the *all* stars observed in short cadence mode (around 2000 in the original *Kepler* mission) may be measured shortly.

A star like the Sun will increase in luminosity by only around a factor of two before turning off the MS. In addition, the Sun's temperature will only increase by around 100 K during its ∼8 billion year MS lifetime. Luminosity and temperature are not sensitive age proxies for Sun-like stars and can also be difficult to measure, with their precision highly sensitive to their distance and the amount of extincting dust along the line of sight. On the other hand, due to magnetic braking the Sun's rotation period will vary by almost an order of magnitude over its MS lifetime. Stellar rotation periods are much more sensitive to age than luminosity or temperature and can be measured precisely with little dependence on distance and none on extinction. Gyrochronology, the dating method that uses stellar rotation periods, has the potential to provide MS star ages that are precise to around 20% (Epstein and Pinsonneault 2014). Due to the abundance of rotation periods of MS stars already provided by *Kepler*/*K2* and the many more expected from future photometric surveys, gyrochronology is one of the most readily available methods for inferring precise stellar ages and, as such, has gained interest over the last few years.

Magnetic braking in MS stars was first observed by Skumanich (1972) who, using observations of young clusters and the Sun, found that the rotation periods of Solar-type stars decay with the square-root of time. It has since been established that the rotation period of a star depends, to first order, only on its age and mass (*e.g.* Barnes 2003). This means that by measuring a star's rotation period and a suitable mass proxy (B-V color is commonly used), one can determine its age. The convenient characteristic of stars that allows their ages to be inferred from their *current* rotation periods and independently of their primordial ones, comes from the steep dependence of spin-down rate on rotation period (Kawaler 1989). Observations of young clusters indicate that stellar angular momentum loss rate is proportional to the cube of the angular velocity. This means that a star spinning with high angular velocity will experience a much greater angular momentum loss rate than a slowly spinning star. For this reason, no matter the initial rotation period of a Sun-like star, after around the age of the Hyades, (∼ 600 Myr) stellar rotation periods appear to converge onto a tight sequence. After this time, the age of a star can be inferred, to first order, from its mass and rotation period alone.

The relation between age, rotation period and mass has been studied in detail CITATIONS, and several different models have been developed to capture the rotational evolution of Sun-like stars. Some of these models are theoretical and based on physical processes; mod-

eling angular momentum loss as a function of the stellar properties, plus the properties of the magnetic field and stellar wind. Other models are empirical and capture the behavior of stars from a purely observational standpoint, using simple functional forms that can reproduce the data. Both types of model; theoretical and empirical, must be calibrated using observations. Even the theoretical models are highly sensitive to some stellar properties that are not measurable: mass-loss rate and magnetic field geometry, for example. However, despite significant advances in both types of model, the gyrochronology relations have not yet been finalized for two main reasons. Firstly, the rotational evolution of stars is complex and not well understood. It is difficult to reproduce the trends in the data using the known physical processes acting within stellar interiors, surfaces and winds. It is also challenging to come up with an empirical model that is flexible enough to capture trends in the data. Secondly, there is a lack of suitable calibration stars with precisely measured ages, particularly at old ages. This region of parameter space is especially important because new evidence suggests that rotational evolution goes through a transition at old age. For example, old *Kepler* asteroseismic stars rotate more rapidly than expected given their age (*e.g.* Angus et al. 2015; van Saders et al. 2016). van Saders et al. (2016) introduced a new, physically motivated, gyrochronology model that can reproduce these data. It relaxes magnetic breaking at a critical Rossby number, *Ro* (the ratio of rotation period to the convective overturn timescale) of around the Solar value, 2.1. This model predicts that, after stellar rotation periods lengthen enough to move stars cross this *Ro* threshold, stars stop spinning down and maintain a constant rotation period from then until they evolve off the MS. The implication is that the ages of stars with $Ro > 2.1$ cannot be measured from their rotation periods.

Despite recent advances in rotation-dating, there is substantial room for improvement in the gyrochronology relations. For example, there is, as yet no *fully* empirical gyrochronology model that includes a weakened magnetic braking law after the $Ro = 2.1$ transition. In addition, no single gyrochronology relation can reproduce the rotational behaviour of all open clusters; the relation between rotation period, age and mass varies from cluster to cluster in a way that cannot be captured by any current model. New asteroseismic calibrators will become available from reprocessed *Kepler* short cadence light curves, however significant numbers of suitable gyrochronology calibrators may not be accessible until after the European Space Agency's *PLATO* mission is launched.

The van Saders et al. (2016) gyrochronology models that capture post *Ro*-threshold, rotational evolution are the state-of-the-art in rotation dating. However, despite their superior accuracy, they are expensive to compute and, just as with most isochrones and stellar evolution tracks, are usually pre-computed over a grid of stellar parameters in order to perform computionally tractable inference. Inferring ages using these models is similar to inferring an age using any set of isochrones, with the main difference being that rotation

period is an additional dimension. Ages calculated using these models are therefore likely to be more precise than using rotation-free isochrones since rotation period provides an additional anchor-point for the age of a star. We present here a complementary method that combines isochrones with an empirical gyrochronology model using a Bayesian framework. The methodology is related to the van Saders et al. (2016) models described above in that both use a combination of rotation periods and other observable properties that track stellar evolution on the HR diagram in concert. The main difference is that the gyrochronology model used here is an entirely empirically calibrated one, as opposed to a physically derived one. One major advantage of using a physically motivated gyrochronology model over an empirically calibrated one is the ability to rely on physics to interpolate or extrapolate over parts of parameter space with sparse data coverage. However, rotational spin-down is a complex process that is not yet fully understood and currently no physical model can accurately reproduce all the data available. For this reason, even physically motivated gyrochronology models cannot always be used to reliably extrapolate into unexplored parameter space. A downside of using a physical model is that it is difficult to build in an element of stochasticity. In other words, rotation period and mass measurements will correspond to a *single* age prediction. On the other hand, it is relatively easy to adjust the level of determinism in empirical gyrochronology relations so that rotation period and mass measurements will lead to a probability distribution over ages. This is a desirable feature of a gyrochronology model because rotational spin-down is a noisy process. In a deterministic model a star with a rotation period that misrepresents its age will have an incorrectly but precisely inferred age. If however, some allowance for outliers or instrinsic scatter is built into the models, such a star would be recognized as an outlier and would have an imprecisely inferred age. Although we use a simple version of an empirical gyrochronology model in this work, which, like any other gyrochronology model, cannot yet reproduce all the observed data, several simple modifications could be made to this model that *would* produce significant improvements. For example, an allowance for outliers; stars with anomalously fast or slow rotation periods, could be build into our model. Ultimately, the model we present here will provide a baseline against which more physically motivated models, e.g. the van Saders et al. (2016) models, can be compared.

There is still some way to go before the models we use to age-date MS stars produce precise and accurate ages. This paper presents an incremental step toward improving age-dating models and best-practises. It also provides a discussion on the balance between accuracy and precision within age-dating models.

This paper is laid out as follows. In section 2 we describe our new age-dating model and its implementation, in section 3 we test this model on simulated stars, cluster stars and asteroseismic stars, and in section 4 we discuss the implications of these tests and future

pathways for development. Throughout this paper we use the word *'observables'* to describe the set of $T_{\rm eff}$, log g, observed bulk metallicity, parallax, photometric color and rotation period observations for a given star. We use the word *'parameters'* to refer to the physical properties of that star: age, mass, true bulk metallicity, distance and V-band extinction that *generate* the observables.

2. Method

A common approach to age-dating a star is to make separate age predictions using separate sets of observables. For example, if the rotation period, parallax and apparent magnitudes in a range of bandpasses were available, one could compute both the gyrochronal age of a star and its isochronal age separately. How these two age predictions are later combined is then a difficult choice. Is it best to average these predictions or just use the more precise of the two, or the one believed to be more accurate? The methodology described here provides an objective method for combining age estimates. There is, after all, only one age for each star. In Bayesian statistics, combining information from different models can be relatively simple, as long as the processes being modeled; those that generated the data, are independent. In this case, we are combining information that relates to the burning of hydrogen in the core (this is the process that drives the slow increase in $T_{\rm eff}$ and luminosity over time) with information about the magnetic braking history of a star (the current rotation period). We can assume that, to first order, these two processes are independent: the hydrogen fraction in the core does not affect a star's rotation period and vice versa. In practise, we can never be entirely sure that two such processes are independent but, at least within the uncertainties, any dependence here is unlikely to affect our results. If this assumption is valid, the likelihoods calculated using each model can be multiplied together.

The desired end product of this method is an estimate of the non-normalized posterior probability density function (PDF) over the age of a star,

$$p(A|\mathbf{m_x}, T_{\rm eff}, \log g, \hat{F}, P, \bar{\omega}), \tag{1}$$

where A is age, $\mathbf{m_x}$ is a vector of apparent magnitudes in various bandpasses (in our model $\mathbf{m_x} = [m_J,\ m_H,\ m_K]$), $\hat{F}$ is the *observed* bulk metallicity, P is the rotation period and $\bar{\omega}$ is parallax. In order to calculate a posterior PDF over age, we must marginalize over parameters that relate to age, but are not of interest in this study: mass (M), distance (D), V-band extinction (A_V) and the *inferred* bulk metallicity, F. The marginalization involves integrating over these extra parameters,

$$\begin{aligned} &p(A|\mathbf{m_x}, T_{\rm eff}, \log g, \hat{F}, P, \bar{\omega}) \\ &\propto \int p(\mathbf{m_x}, T_{\rm eff}, \log g, \hat{F}, P, \bar{\omega}|A, M, D, A_V, F)\ p(A)p(M)p(D)p(A_V)p(F)dMdDdA_VdF. \end{aligned} \tag{2}$$

This equation is a form of Bayes' rule,

$$\text{Posterior} \propto \text{Likelihood} \times \text{Prior}, \tag{3}$$

where the likelihood of the data given the model is,

$$p(\mathbf{m_x}, T_{\rm eff}, \log g, \hat{F}, P, \bar{\omega}|A, M, D, A_V, F), \tag{4}$$

and the prior PDF over parameters is,

$$p(A)p(M)p(D)p(A_V)p(F). \tag{5}$$

Not all of the observables on the left of the '|' in the likelihood depend on all of the parameters to the right of it. For example, rotation period, P doesn't depend on V-band extinction, A_V. In our model, we make use of conditional independencies like this and use them to factorize the likelihood. Instead of the likelihood we wrote in equation 3, where every observable depends on every parameter, our model can be factorized as,

$$p(\mathbf{m_x}, T_{\rm eff}, \log g, \hat{F}, \bar{\omega}, C_{B-V}|A, M, D, A_V, F)\ p(P|A, C_{B-V}), \tag{6}$$

where we have introduced a new parameter, C_{B-V}, which is the $B-V$ color that is often used as a mass proxy in the literature. In our model C_{B-V} is not measured but *inferred*: it is a latent parameter. We infer C_{B-V} because all *Kepler* stars have 2MASS photometry in J, H and K bands but do not all have B and V band colors. However, the gyrochronology model we use is calibrated to B-V color, not J-K or otherwise. A probabilistic graphical model (PGM) depicting the joint probability over parameters and observables is shown in figure 1. It describes the conditional dependencies between parameters (in white circles) and observables (in grey circles) with arrows leading from the causal processes to the dependent processes. For example, it is the mass, age, metallicity, extinction and distance that determines the observed spectroscopic properties ($T_{\rm eff}$, log g and [Fe/H]) and apparant magnitudes (m_J, m_H and m_K). These parameters also determine the B-V color of a star. In turn, it is a star's age and B-V color that determine its rotation period. Note that, written this way, stellar rotation periods do not directly depend on stellar mass. Mass determines C_{B-V} and C_{B-V}, along with age determines rotation period. The purpose of this PGM is not to depict the physical realities of stellar evolution, it is only a visual description of the structure of the model *we* use here. Braking up the problem this way allows us to efficiently join isochronology and gyrochronology and infer the joint age of a star from all its observables. It may well be that rotation period depends directly on mass and metallicity in reality, but it is more practical for us to assume that these dependencies are weak enough not to significantly affect the ages that we ultimately infer.

The factorization of the likelihood described in equation 6 and depicted in figure 1 allows us to multiply two separate likelihood functions together: one computed using an isochronal model and one computed using a gyrochronal model. We assume that the probability of observing the measured observables, given the model parameters is a Gaussian and that the observables are identically and independently distributed. These assumptions allow us to use Gaussian likelihood functions. The isochronal likelihood function is,

$$\mathcal{L}_{\rm iso} = p(\mathbf{m_x}, T_{\rm eff}, \log g, \hat{F}, \bar{\omega}, C_{B-V}|A, M, D, A_V, F) \tag{7}$$

Fig. 1.— A probabilistic graphical model (PGM) showing the conditional dependencies between the parameters (white nodes) and observables (gray nodes) in our model. Apparent magnitude, m_x, effective temperature, $T_{\rm eff}$, surface gravity, log g, observed bulk metallicity, $\hat{F}$, and parallax, $\bar{\omega}$ are determined by the mass, M, age, A, distance, D, extinction, A_V and bulk metallicity, F, of a star. These dependencies are indicated by arrows that start at a 'parent' node and end at the dependent observable, or 'child' node. The box drawn around some of the nodes indicates that everything inside it depends on every parameter that points toward it. For example, log g depends on A, M, D, A_V, and F. In our model, rotation period, P, only depends on age and a B-V color that is a latent parameter, predicted from the isochronal model. In our model, rotation period does not directly depend on distance, extinction, metallicity or mass, only age and B-V color. This PGM is a representation of the factorized joint PDF over parameters and observables which is written in equation **??**.

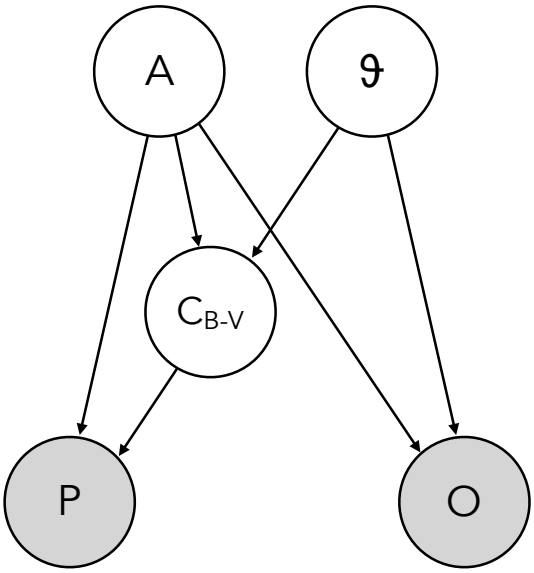

$$= \frac{1}{\sqrt{(2\pi)^n \det(\Sigma)}} \exp\left(-\frac{1}{2}(\mathbf{O_I} - \mathbf{I})^T \Sigma^{-1} (\mathbf{O_I} - \mathbf{I})\right),$$

where $\mathbf{O_I}$ is the vector of n observables: $T_{\rm eff}$, log g, $\hat{F}$, $\bar{\omega}$, m_j, m_h and $m_k$and Σ is the covariance matrix of that set of observables. $\mathbf{I}$ is the vector of *model* observables that correspond to a set of parameters: A, M, F, D and A_V, calculated using an isochrone model. We assume there is no covariance between these observables and so this covariance matrix consists of individual parameter variances along the diagonal with zeros everywhere else. The gyrochronal likelihood function is,

$$\mathcal{L}_{\rm gyro} = p(P|A, C_{B-V}) \tag{8}$$
$$= \frac{1}{\sqrt{(2\pi)\det(\Sigma_P)}} \exp\left(-\frac{1}{2}(\mathbf{P_O} - \mathbf{P_P})^T \Sigma^{-1} (\mathbf{P_O} - \mathbf{P_P})\right),$$

where $\mathbf{P_O}$ is a 1-D vector of observed rotation periods, $\mathbf{P_P}$ is the vector of corresponding predicted rotation periods, calculated using the vector of inferred ages and C_{B-V} values predicted by the isochronal model. The full likelihood function used in our model is the product of these two likelihood functions,

$$\mathcal{L}_{\rm full} = \frac{1}{\sqrt{(2\pi)^n \det(\Sigma)}} \exp\left(-\frac{1}{2}(\mathbf{O_I} - \mathbf{I})^T \Sigma^{-1} (\mathbf{O_I} - \mathbf{I})\right) \tag{9}$$
$$\times \frac{1}{\sqrt{(2\pi)\det(\Sigma_P)}} \exp\left(-\frac{1}{2}(\mathbf{P_O} - \mathbf{P_P})^T \Sigma^{-1} (\mathbf{P_O} - \mathbf{P_P})\right).$$

We place priors over the model parameters A, M, F, D and A_V. These priors represent our 'prior beliefs' about the values these parameters will take, before we use the data to update those beliefs via a likelihood and produce a 'posterior' belief about their values. These priors are described in the appendix.

The gyrochronology model we use to predict P_P is,

$$P = A^\eta \alpha (B - V - \delta)^\beta, \tag{10}$$

where η, α, β and δ take values 0.55, 0.4, 0.31 and 0.45 respectively. These values are adopted from the recalibration performed in **?** that uses young cluster stars and old asteroseismic stars and incorporates a mixture model that prevents outliers from influencing the fit. In **?** it was found that the old asteroseismic stars could not be fit using the above functional form. Subsequently, van Saders et al. (2016) discovered that the magnetic braking of these old stars has ceased and cannot be modeled with a Skumanich-like spin-down law. In future, the above model should be updated to a broken power law, or similar, in order to account for the change in slope of the rotation period-age relation. Until then, this method should only be used for stars below the Rossby number threshold, *i.e.* who's rotation period to convection overturn time ratio ($P/\tau = Ro$) does not exceed 2.1 (van Saders et al. 2016). In this work we do not

seek to recalibrate the gyrochronology models, but simply to introduce this new framework where rotation periods are modeled simultaneously with isochronal features. Although this gyrochronology model does not provide a good fit to all the available data, we reiterate that no single model *is* able to reproduce all the data, and that there is utility in using an extremely simple functional form like this. Again, this is not meant as a calibration exercise: in this paper we are more concerned with introducing a new approach to modeling stellar ages, however, our method is highly flexible and modular and an improved gyrochronology model could easily be swapped in for this one in future.

To calculate $\mathbf{I}$, the vector of predicted isochronal observables, we use the `isochrones.py` *python* package which has a range of functionalities relating to isochrone fitting. The first of the `isochrones.py` functions we use is the likelihood function of equation 8. The `isochrones.py` likelihood function accepts a dictionary of observables which can, but does not *have* to include, all of the following: $T_{\rm eff}$, log g, [Fe/H], parallax and apparent magnitudes in a range of colors, as well as the uncertainties on all these observables. It then calculates the residual vector $(\mathbf{O_I} - \mathbf{I})$ where $\mathbf{O_I}$ is the vector of observables and $\mathbf{I}$ is a vector of corresponding predicted observables. The prediction is calculated using a set of isochrones (we use the MIST models **?**), where the set of *model* observables that correspond to a set of physical parameters is returned. This requires interpolation over the model grids since, especially at high dimensions, it is unlikely that any set of physical parameters will exactly match a precomputed set of isochrones. The observables that correspond to a set of physical parameters (age, mass, etc) go into $\mathbf{I}$ and the `isochrones.py` likelihood function returns the result of equation 8. The second `isochrones.py` function we use is one that querys the best-fit isochrone model chosen to predict $\mathbf{I}$, in order to predict the corresponding C_{B-V} for that star. This color is then used to calculate the gyrochronal likelihood function of equation 9.

The inference processes procedes as follows (as a reminder, we use *observables* to refer to the data: $T_{\rm eff}$, log g, etc and *parameters* to refer to the model parameters: age, mass, etc). First, a set of parameters: age, mass, true bulk metallicity, distance and extinction, as well as observed values of $T_{\rm eff}$, log g, bulk metallicity, 2MASS colors and parallax ($\mathbf{O_I}$) for a single star are passed to the isochronal likelihood function (equation 8). Then, a set of *model* values of $T_{\rm eff}$, log g, bulk metallicity, 2MASS colors and parallax ($\mathbf{I}$) that correspond to that set of parameters are calculated by `isochrones.py`. The isochronal log-likelihood, $\ln(\mathcal{L}_{\rm iso})$, is then computed for these parameter values. The same age that was passed to the likelihood function, and the C_{B-V} corresponding to it, along with the observed rotation period, are then passed to the gyrochronal likelhood function (equation 9). The gyrochronal log-likelihood, $\ln(\mathcal{L}_{\rm gyro})$, is computed. The full log-likelihood is then calculated: $\ln(\mathcal{L}_{\rm full}) = \ln(\mathcal{L}_{\rm iso}) + \ln(\mathcal{L}_{\rm gyro})$ and added to the log-prior to produce a single sample from

the posterior PDF.

We sample the joint posterior PDF over age, mass, metallicity, distance and extinction using the affine invariant ensemble sampler, `emcee` (**?**). 24 walkers are used with 15,000 burn-in steps followed by 25,000 full-run steps. This provides a total of $25,000 \times 24 = 600,000$ non-independent samples. In order to assess convergence we calculate the autocorrelation time of each MCMC chain. The method described above is embarassingly parallelizable, since the physical parameters of each star can be inferred on a separate node. Running our code on a cluster, we found that a posterior PDF can be estimated for a single star in around one minute.

3. Results

In order to demonstrate the functionality of our method, we conduct a series of tests. In the first we simulate a set of observables from a set of fundamental parameters for a few hundred stars using the MIST (**?**) stellar evolution models. In the second we test our model by attempting the measure the ages of stars in known clusters who's ages have been established through ensemble isochrone fitting and MS turn-off. In the third test we compare our ages with those of asteroseismic measurements for around twenty stars.

For the first test we began with a set of 1000 stars and drew masses, ages, bulk metallicities, distances and extinctions at random from the following uniform distributions:

$$M \sim U(0.5, 1.5)\ [M_\odot] \tag{11}$$
$$A \sim U(0.5, 14)\ [\mathrm{Gyr}] \tag{12}$$
$$F \sim U(-0.2, 0.2) \tag{13}$$
$$D \sim U(10, 1000)\ [\mathrm{pc}] \tag{14}$$
$$A_V \sim U(0, 1). \tag{15}$$

$T_{\rm eff}$, log g, $\hat{F}$, m_x, $\bar{\omega}$ and B-V were then generated using these stellar parameters with the MIST stellar evolution models (**?**) and rotation periods, P were generated from the gyrochronology relation in equation 10 with age, A, and B-V. We then performed cuts on these simulated stars to remove evolved stars and stars that are too hot. The rotation periods of evolved stars, defined here to be those with log g ¿ 4.5 begin to increase as soon as they turn off the MS and their radii start to enlarge and cannot be modeled with the gyrochronology relation of equation 10. In addition, hot stars (defined as 6250 K ¡ $T_{\rm eff}$) cannot be modeled using equation 10 because their convective envelopes are extremely shallow and their magnetic fields are weaker, leading to a lack of magnetic braking. The rotation periods of these stars do not increase substantially during their time on the MS. After performing these cuts, 649 update stars remain in the sample of simulated stars. We attempted to measure their true periods using our method outlined in section **??**. For all stars, our initial guesses for the parameters are $M = 1 M_\odot$, $A = 1$ Gyr, $F = 0$, $D = 500$ pc and $A_V = 0.1$.

The top panel of figure **??** shows the results of using a *purely isochrone* model to estimate the posterior PDFs over the stellar ages of simulated stars. The rotation periods of stars have not been incorporated into this model, these posterior PDFs were obtained by isochrone fitting only. In some cases (shown as points with large errorbars) there is no constraint on the stellar age: the age of the star is consistent with all ages from 0-14 Gyrs. The reason for this is that the temperatures and luminosities of stars do not change very much on the

main sequence. The isochrones are tightly spaced in the MS region of the HR-diagram and, as a result, even precisely measured temperatures and luminosities often do not yield precise ages. In other cases there is a moderate constraint on the age.

In the second panel of figure **??** the results of simply using a gyrochronology model are demonstrated. These ages have been *inferred* using the likelihood of equation 9, rather than calculated by plugging numbers into the gyrochronology relation of equation 10. This means that uncertainties on the rotation periods are propagated through to the posterior. For this experiment, the B-V colors were pre-computed using the MIST isochronal model grid, rather than being jointly inferred at the same time as the ages. Again, the true stellar ages are plotted on the x-axis and the median values of the recovered PDFs over ages are plotted on the y-axis. Here, unlike in the pure isochrone fitting case, the recovered ages are precise. That is because, in the gyrochronology model, age is the only free parameter as opposed to the isochrone model demonstrated in the top panel which has five free parameters: age, mass, metallicity, distance and extinction *and* these parameters are highly correlated. It is also because gyrochronology isochrones (or gyrochrones) are more widely separated relative to the observational uncertainties than the isochrones used above. In addition, there is no intrinsic scatter built into this gyrochronology model; it is deterministic. This means that the pair of measurements: rotation period and B-V, returns a single-valued age, rather than a probability distribution over ages. Because we are testing the gyrochronology-only model on *simulated* data, these results look precise *and* accurate, but that is misrepresentive. Inaccuracies would arise if the gyrochronology were incorrect or not precisely calibrated in all parts of parameter space which is in fact the case in reality. However, since we simulated these data from the same model we used to recover the ages, the resulting ages inferred are accurate by construction.

The third panel of figure **??** shows the perfect middle ground between precise but inaccurate gyrochronology and accurate but imprecise isochrone models.

Although inferred ages are likely to be more precise if spectroscopic parameters are available ($T_{\rm eff}$, log g and [Fe/H]), it is still possible to place constraints on stellar ages if only photometric colors are available, especially if the star has a precise parallax measurement. Figure **??** demonstrates the decrease in precision when only photometric colors (J, H and K), parallaxes and rotation periods are used as observables. The top panel of figure **??** shows an isochrones-only model and the bottom panel shows the results of using isochrones *and* gyrochronology. When spectroscopic parameters are not available, including age information from a stellar rotation period becomes extremely important as it is far more age-sensitive than photometric colors. The trade-off, however, is that stellar ages will become gyrochronology dominated, and it is even more important to use an accurate gyrochronology model.

In order to test our model on real stars with known ages, we selected a sample of cluster stars with spectroscopic parameters and rotation periods. We use a sample of Hyades members with spectroscopic parameters ($T_{\rm eff}$, log g and bulk metallicity) from **?**, *K2* rotation periods from **?** and parallaxes from *Gaia*. Note that the age of the Hyades is generally measured using stellar evolution/isochrone models where the ensemble of stars at the same age but a *range of masses* allows a very precise isochronal age to be inferred. In particular, this allows the main sequence-turn off to be identified which, since it appears as a sharp feature in a mono-age population, allows the age of the population to be precisely inferred. In this experiment we do not force the Hyades members to have the same age. We are instead using these stars to reveal the spread in recovered ages and identify regions of parameter space where the predicted ages deviate from the established age for the Hyades (in other words, the precision and accuracy of our method).

The results are shown in figure **??** which follows the same layout as figure **??**. The top panels shows the ages inferred using an isochrone-only model, the middle shows a gyrochrone-only model and the bottom shows an isochrone plus gyrochrone model. Once again, the top panel demonstrates that using an isochrone model alone produces imprecise ages. The middle panel shows ages recovered using only a gyrochronal model and it reveals inaccuracies in the gyrochronology relation used here.

The bottom panel, once again, demonstrates the power of using both isochronal and gyrochronal models together to provide a balance of precision and accuracy.

4. Discussion

In the previous section we demonstrated that modeling the ages of stars using isochrones *and* gyrochronology can result in more precise and accurate ages than using either isochrone fitting or gyrochronology alone.

Isochrone fitting and gyrochronology are extremely complementary because gyrochronology is more precise where isochrone fitting is less precise and vice versa. Age precision is determined by the spacing of isochrones or gyrochrones: in regions where iso/gyrochrones are more tightly spaced, ages will be less precise. Isochrones get less tightly spaced (and more precise) at larger stellar masses and gyrochrones get more tightly spaced (and less precise) at larger stellar masses. Figure **??** shows our simulated star sample on an H-R diagram. Points are positioned by their true properties, not their inferred ones, and colored by their age *precision* as calculated using isochrones and gyrochronology. Paler stars have less precise inferred ages.

Our focus so far has been on stellar age because this is the most difficult stellar parameter to measure. However, if the age precision is improved, then the mass, [Fe/H], distance and extinction precision must also be improved, since these parameters are strongly correlated and co-dependent in the isochronal model. Figure **??** shows the improvement in relative precision of mass measurements from our simulated star sample.

The method we present here will be useful for a large number of stars: any cool, MS star with a measurable rotation period. This number is already in the tens-of-thousands from *Kepler* alone and will be expanded with *TESS*, *LSST*, *WFIRST*, *PLATO*, *Gaia*, *PanSTARRS* and more. However, there are also several types of star for which gyrochronology is, in general, *not* useful. This list includes: stars with thin convective envelopes, more massive than around 1 $M_{\odot}$; fully convectives stars, less massive than around 0.3 $M_{\odot}$; evolved stars with log g less than around 4.5; stars that haven't converged onto the rotational main sequence, *i.e.* those younger than around 500 Myrs; stars who have ceased magnetic braking, *i.e.* those with Ro greater than around 2.1; synchronised binaries who's rotation periods are locked to their orbital periods; and other classes of gyrochronal outliers. Since many stars with measurable rotation periods do not have precise spectroscopic properties, it is not always possible to tell whether a star falls within these permissable ranges of masses, surface gravities and rossby numbers. In addition, any given star, even if it does meet the criteria for mass, evolutionary stage, age, binarity, etc, may still be a rotational outlier. Rotational outliers are often seen in clusters (see *e.g.* **?**). In any case where a star's age is not truly represented by its rotation period, its isochronal age will be in tension with its gyrochronal one. However, given the precision of the gyrochronal technique, the gyrochronal age may dominate over the isochronal one. Figure **??** shows the posterior PDF for a star with a

misrepresentative rotation period. This star is rotating more rapidly than its age and mass indicate it should, so the gyrochronal age of this star is under-predicted. Situations like this are likely to arise relatively often, partly because rotational spin-down is not a perfect process and some unknown physical processes can produce outliers, and partly because misclassified giants, hot stars, M dwarfs or very young or very old stars will not have rotation periods that relate to their ages in the same way. In addition, measured rotation periods may not always be accurate and in many cases, due to aliasing, can be a harmonic of the true rotation period. One of the more common rotation period measurement failure modes is to measure half the true rotation period. The best way to prevent an erroneous or outlying rotation period from resulting in an erroneous age measurement is to *allow* for outlying rotation periods using a mixture model.

Throughout this manuscript we have referred to the 'accuracy' of the isochronal models. In reality though, stellar evolution models are not 100% accurate and different stellar evolution models, *e.g.*, MIST, Dartmouth, Yonsei-Yale, etc will predict slightly different ages. The disagreement between these models varies with position on the HR diagram, but in general, ages predicted using different stellar evolution models will vary by around 10%. We use the MIST models in our code because they cover a broader range of ages, masses and metallicities than the Dartmouth models.

5. Conclusion

We have presented a statistical framework for joining together observations of different stellar properties that relate, via different evolutionary processes, to stellar age. Specifically, we combine information used to place stars on an isochrone in an HR diagram: $T_{\rm eff}$, log g, observed bulk metallicity, parallax and photometric colors with rotation periods, used to date stars via their magnetic braking history. The two methods of ischrone fitting and gyrochronology are simply combined by taking the product of two likelihood functions: one that contains an isochronal model and the other a gyrochronal one. The isochronal model is based on the MIST stellar evolution model (**?**) and computed using `isochrones.py`. The gyrochronal model is a simple 2-dimensional power-law relation between rotation period, B-V color and age. It is based on the functional form first introduced by Barnes (2003) and later recalibrated by **?**.

We tested this age-dating model on simulated data, cluster stars and asteroseismic stars with precisely measured ages. We found that this model predicts ages that are an order of magnitude more precise than using isochrone fitting alone. However, we caution users of this method that our choice of gyrochronology model is not suitable for stars outside a specific range of stellar parameters, described in the text.

In the future we hope to make several improvements to the gyrochronology relation used here, including, allowing for outliers via a mixture model, including intrinsic scatter and/or replacing the power-law with a semi-parametric model.

The code used in this project is available as a documented *python* package called `chronology`. It is available for download on Github or through Pypi (pip install chronology). The documentation is available at readthedocs..... The exact version used to produce the results here is available under add github hash.

6. Appendix

Priors

We use the default priors in the `isochrones.py` *python* package. The prior over age is,

$$p(A) = \frac{\log(10)10^A}{10^{10.5} - 10^8}, \quad 8 < A < 10.5. \tag{16}$$

where A, is $\log_{10}$(Age [yrs]). The prior over mass is uniform in natural-log between -20 and 20,

$$p(M) = U(-20, 20) \tag{17}$$

where M is ln(Mass $[M_\odot]$). The prior over true bulk metallicity is based on the galactic metallicity distribution, as inferred using data from the Sloan Digital Sky Survey citation. It is the product of a Gaussian that describes the metallicity distribution over halo stars and two Gaussians that describe the metallicity distribution in the thin and thick disks:

$$\begin{aligned} p(F) = & \quad H_F \frac{1}{\sqrt{2\pi\sigma^2_{\rm halo}}} \exp\left(-\frac{(F-\mu_{\rm halo})^2}{2\sigma_{\rm halo}}\right) \\ & \times (1 - H_F)\frac{1}{\xi}\left[\frac{0.8}{0.15}\exp\left(-\frac{(F-0.016)^2}{2\times 0.15^2}\right) + \frac{0.2}{0.22}\exp\left(-\frac{(F-0.15)^2}{2\times 0.22^2}\right)\right], \end{aligned} \tag{18}$$

where $H_F = 0.001$ is the halo fraction, $\mu_{\rm halo}$ and $\sigma_{\rm halo}$ are the mean and standard deviation of a Gaussian that describes a probability distribution over metallicity in the halo, and take values -1.5 and 0.4 respectively. The two Gaussians inside the square brackets describe probability distributions over metallicity in the thin and thick disks. The values of the means and standard deviations in these Gaussians are from **?**. ξ is the integral of everything in the square brackets from $-\infty$ to ∞ and takes the value ~ 2.507. The prior over distance is,

$$p(D) = \frac{3}{3000^3} D^2, \quad 0 < D < 3000, \tag{19}$$

where D is in kiloparsecs. Finally, the prior over extinction is uniform between zero and one,

$$p(A_V) = U(0, 1). \tag{20}$$

Some of the data presented in this paper were obtained from the Mikulski Archive for Space Telescopes (MAST). STScI is operated by the Association of Universities for Research in Astronomy, Inc., under NASA contract NAS5-26555. Support for MAST for non-HST data is provided by the NASA Office of Space Science via grant NNX09AF08G and by other grants and contracts. This paper includes data collected by the Kepler mission. Funding for the Kepler mission is provided by the NASA Science Mission directorate.

REFERENCES

R. Angus, S. Aigrain, D. Foreman-Mackey, and A. McQuillan. Calibrating gyrochronology using Kepler asteroseismic targets. *MNRAS*, 450:1787–1798, June 2015. doi: 10.1093/mnras/stv423.

S. A. Barnes. On the Rotational Evolution of Solar- and Late-Type Stars, Its Magnetic Origins, and the Possibility of Stellar Gyrochronology. *ApJ*, 586:464–479, March 2003. doi: 10.1086/367639.

C. R. Epstein and M. H. Pinsonneault. How Good a Clock is Rotation? The Stellar Rotation-Mass-Age Relationship for Old Field Stars. *ApJ*, 780:159, January 2014. doi: 10.1088/0004-637X/780/2/159.

S. D. Kawaler. Rotational dating of middle-aged stars. *ApJ*, 343:L65–L68, August 1989. doi: 10.1086/185512.

A. Skumanich. Time Scales for CA II Emission Decay, Rotational Braking, and Lithium Depletion. *ApJ*, 171:565, February 1972. doi: 10.1086/151310.

J. L. van Saders, T. Ceillier, T. S. Metcalfe, V. Silva Aguirre, M. H. Pinsonneault, R. A. García, S. Mathur, and G. R. Davies. Weakened magnetic braking as the origin of anomalously rapid rotation in old field stars. *Nature*, 529:181–184, January 2016. doi: 10.1038/nature16168.